JCB Article

A role for cofilin and LIM kinase in *Listeria*-induced phagocytosis

Hélène Bierne,[1] Edith Gouin,[1] Pascal Roux,[2] Pico Caroni,[3] Helen L. Yin,[4] and Pascale Cossart[1]

[1]Unité des Interactions Bactéries-Cellules, and [2]Station de Microscopie Confocale, Institut Pasteur, 75724 Paris Cedex 15, France
[3]Friedrich Miescher Institute, CH-4058 Basel, Switzerland
[4]University of Texas, Southwestern Medical Center, Dallas, TX 75390

The pathogenic bacterium *Listeria monocytogenes* is able to invade nonphagocytic cells, an essential feature for its pathogenicity. This induced phagocytosis process requires tightly regulated steps of actin polymerization and depolymerization. Here, we investigated how interactions of the invasion protein InlB with mammalian cells control the cytoskeleton during *Listeria* internalization. By fluorescence microscopy and transfection experiments, we show that the actin-nucleating Arp2/3 complex, the GTPase Rac, LIM kinase (LIMK), and cofilin are key proteins in InlB-induced phagocytosis. Overexpression of LIMK1, which has been shown to phosphorylate and inactivate cofilin, induces accumulation of F-actin beneath entering particles and inhibits internalization. Conversely, inhibition of LIMK's activity by expressing a dominant negative construct, LIMK1$^-$, or expression of the constitutively active S3A cofilin mutant induces loss of actin filaments at the phagocytic cup and also inhibits phagocytosis. Interestingly, those constructs similarly affect other actin-based phenomenons, such as InlB-induced membrane ruffling or *Listeria* comet tail formations. Thus, our data provide evidence for a control of phagocytosis by both activation and deactivation of cofilin. We propose a model in which cofilin is involved in the formation and disruption of the phagocytic cup as a result of its local progressive enrichment.

Introduction

Pathogenic bacteria exploit key cell functions to establish infections and have proven to be instrumental in deciphering some fundamental cellular processes such as actin-based motility (Finlay and Cossart, 1997; Cossart, 2000). Several bacteria are able to induce their own uptake by nonprofessional phagocytes and appear as tools of choice to analyze phagocytosis. Among those, *Listeria monocytogenes* is an intracellular pathogen able to invade a wide variety of cells and disseminate from cell to cell via an actin-based motility (for review see Cossart and Bierne, 2001). The *Listeria*-induced phagocytosis process is initiated by intimate contact between bacterial invasion proteins and host cell receptors and is followed by the progressive engulfment of the bacterial body into the target cell, a so-called "zipper-like" mechanism. Two invasion proteins, InlA (also called internalin) and InlB, play a key role in this process. InlA mediates entry into cells expressing its receptor E-cadherin (Mengaud et al., 1996a). InlB promotes entry into various cell types including hepatocytes, epithelial, and endothelial cells. InlB was identified recently as a ligand of Met, the hepatocyte growth factor (HGF)*/scatter factor receptor, and InlB–Met interactions are critical for *L. monocytogenes* entry into epithelial cells (Shen et al., 2000). InlB also interacts with gC1qR, an ubiquitous glycoprotein, which could act as a coreceptor for Met (Braun et al., 2000). The InlB-mediated signaling responses are comparable to those triggered by HGF and include tyrosine phosphorylations and phosphatidylinositol 3-kinase and PLC-γ1 activation (Ireton et al., 1996; Bierne et al., 2000; Shen et al., 2000).

The links between activation of InlB receptors and the transient actin polymerization and depolymerization steps required for internalization are poorly understood. Interestingly, like HGF, soluble InlB mediates membrane ruffling in some cell types (Ireton et al., 1999). Membrane ruffling or lamellipodia formation induced by other stimuli require the coordinate action of the small GTPases Rac1 and Cdc42 (Ridley and Hall, 1992; Cox et al., 1997), the Arp2/3 complex (Bailly et al., 1999; Svitkina and Borisy, 1999),

Address correspondence to Pascale Cossart, Unite des Interactions Bacteries-Cellules, Institut Pasteur, 28 rue du Dr Roux, 75724 Paris Cedex 15, France. Tel.: 33-1-45-68-88-41. Fax: 33-1-45-68-87-06. E-mail: pcossart@pasteur.fr

Key words: *Listeria monocytogenes*; cytoskeleton; Met; InlB; actin-based motility

*Abbreviations used in this paper: ADF, actin depolymerizing factor; HGF, hepatocyte growth factor; LIMK, LIM kinase; PFA, paraformaldehyde.

and proteins belonging to the actin depolymerizing factor (ADF)/cofilin family (Meberg et al., 1998; Svitkina and Borisy, 1999; Chan et al., 2000). The Arp2/3 complex regulates the actin filament network by promoting actin filament nucleation and branching (for review see Welch, 1999; Cossart, 2000). ADF/cofilin enhances the rate of actin turnover by both severing actin filaments (F-actin), thereby creating new filament barbed ends, and increasing actin depolymerization at free pointed ends, providing a pool of actin monomers for F-actin assembly (for review see Bamburg, 1999; Chen et al., 2000). Cofilin is inactivated by phosphorylation on serine 3, which prevents its association with actin, and reactivated by dephosphorylation. Therefore, filament turnover is regulated by a cofilin phosphocycle. LIM kinase (LIMK) catalyses phosphorylation of cofilin on serine 3, and its overexpression into cells reverses cofilin-induced actin depolymerization, leading to accumulation of actin filaments and aggregates (Arber et al., 1998; Yang et al., 1998).

In this work, we investigated whether factors involved in ruffle formation in other systems were involved not only in InlB-induced ruffling but also in InlB-induced "zipper-like" phagocytosis. By a series of colocalization and functional experiments, we first provide evidence that these processes are dependent on the Arp2/3 complex. Then, we show that cofilin, LIMK, and Rac are essential for InlB-mediated cytoskeleton rearrangements, highlighting the role of the cofilin phosphocycle in internalization. Our results support a model in which cofilin not only stimulates actin polymerization events, allowing internalization or ruffling, but also controls filament disassembly at the phagocytic cup, a step crucial for an efficient entry process.

Results

Kinetics of InlB-mediated internalization: actin and Met recruitment

The process of *Listeria* internalization into nonphagocytic cells can be divided into several stages: (a) contact of extracellular bacteria with the cell, (b) formation of the phagocytic cup, which involves membrane extension and actin polymerization, (c) closure of the phagocytic cup, and (d) disassembly of actin filaments (F-actin) around the newly formed vacuole containing the intracellular bacterium (Fig. 1 A). Internalized *Listeria* are then released into the cytoplasm after lysis of the vacuole. To analyze the kinetics of this induced phagocytosis, when promoted by the InlB protein, we monitored entry of InlB-coated latex beads, which are efficiently internalized in the absence of any other listerial factors (Braun et al., 1998), and entry of bacteria. Since entry of the wild-type *L. monocytogenes* strain EGD is relatively inefficient, we used a hyperinvasive variant strain, EGDΔ*inlB*(LRRs-IR-SPA). This variant expresses an InlB derivative containing the NH_2-terminal region sufficient for entry (LRRs-IR domains), which is covalently anchored at the bacterial surface (Braun et al., 1999). The resulting strain is ~40-fold more invasive than the wild-type strain in Vero cells in which *Listeria* is internalized solely by the InlB pathway (unpublished data).

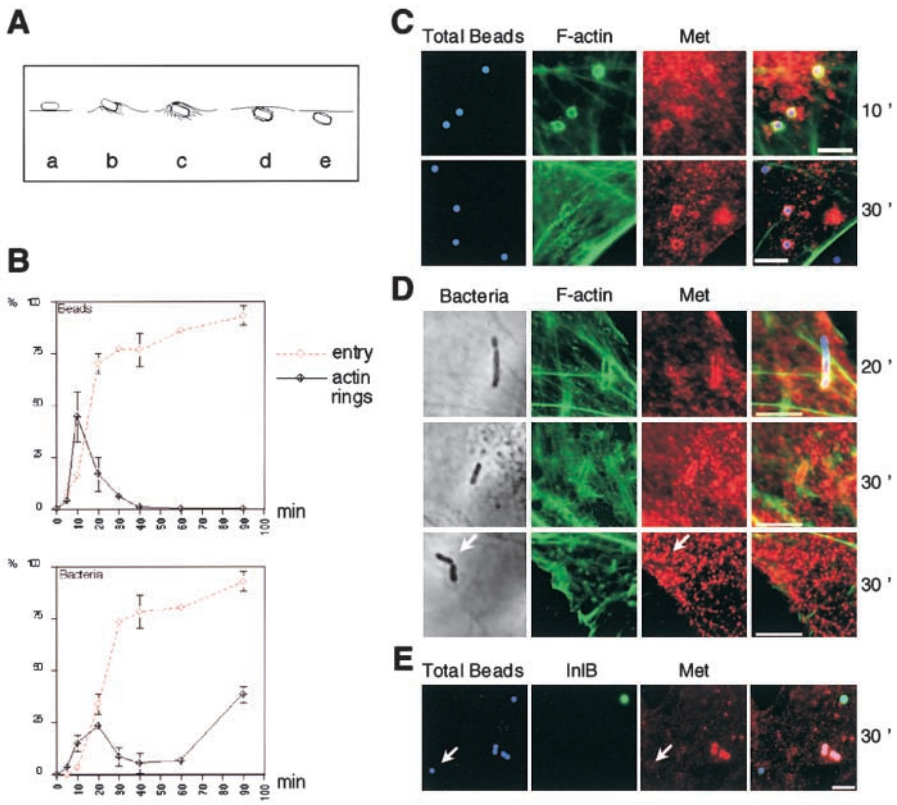

Figure 1. **Actin and Met recruitment during InlB-mediated internalization.** (A) Diagram of the internalization process: adherent bacteria (a), formation of the phagocytic cup with actin polymerization (b), phagocytic cup closure (c), disruption of the F-actin cup with residual (d) or no (e) F-actin around the phagosome. (B) Kinetic analysis of F-actin cup formation during InlB-mediated entry. Internalized and F-actin–associated InlB particles were quantified by immunofluorescence at different times after infection. Results are expressed as the percentage of intracellular particles (red dashed line) or the percentage of particles associated with an F-actin ring (black solid line) among the total number of cell-associated particles. (C–E) Met recruitment during InlB bead or bacteria entry at different times after infection. (C) Vero cells were stained with FITC-phalloidin (green) and anti-Met Ab (red). InlB beads are intrinsically fluorescent (blue). (D) Total bacteria associated with cells were visualized in phase–contrast, and bacteria that are fully or partly extracellular were detected by labeling with anti-InlA Ab before cell permeabilization (last panel, blue). (E) Extracellular beads were labeled with anti-InlB Ab (green) before cell permeabilization. Arrows indicate intracellular InlB beads or bacteria not associated with Met. Bars, 5 μm.

The kinetics of entry were analyzed in Vero cells by following the appearance of intracellular and F-actin–associated particles after shifting infected cells from 4 to 37°C. InlB bead internalization started 5 min after the temperature shift and reached 75% after 20 min, whereas entry of bacteria occurred mainly between 10 and 30 min after the shift, suggesting that the rate of bacterial entry is slower than that of beads (Fig. 1 B). However, the final efficiency of bacteria and bead entry was identical 1 h after infection (80% of internalized particles for a moi of 5:1). The formation of an F-actin ring beneath beads and bacteria peaked 10 (Fig. 1 C) and 20 min (Fig. 1 D) after infection, respectively. Subsequently, this F-actin ring was replaced by a residual punctuated F-actin labeling, no longer intense and uniform as at earlier times, around the beads or bacteria trapped into phagosomes or disappeared completely around bacteria that presumably have escaped from the phagocytic vacuole. A new increase in the number of F-actin–associated bacteria occurred 60 min after infection (Fig. 1 B). It corresponds to *Listeria* that have escaped from the vacuole and start recruiting and polymerizing actin for intracellular movement.

We determined whether actin polymerization during internalization was concomitant with recruitment of the Met receptor, which is critical for InlB-mediated entry into Vero cells. Met was detected around all entering beads or bacteria associated with F-actin rings at the entry peak at 10 or 20 min, respectively (Fig. 1, C and D). Then, at 30 min when most of the internalization process is achieved particles that were still labeled with Met antibodies displayed a residual punctuated F-actin staining. At that time, ~70% of intracellular bacteria (Fig. 1 D) and 30% of intracellular beads (Fig. 1 E) were no longer associated with Met, possibly after Met recycling or in the case of bacteria after lysis of the vacuole. Thus, these colocalization studies indicate that actin dynamics during InlB-mediated internalization can be analyzed within 30 min after infection and independently of the *Listeria* actin-based movements.

A role for Arp2/3 in InlB-mediated membrane ruffling and entry

The Arp2/3 complex is involved in membrane ruffles and lamellipodia formation induced by PDGF or EGF stimulation (Machesky and Insall, 1998; Bailly et al., 1999). We examined whether it was also involved in the formation of InlB-mediated membranes ruffles. Treatment of Vero cells with 4.5 nM InlB induces formation of membrane ruffles in 82 ± 6% of the cells, whereas only 5% of untreated cells showed such structures as reported previously (Ireton et al., 1999). Arp3 was detected in these InlB-induced membranes ruffles and colocalized with F-actin (Fig. 2 A). To analyze the role of Arp2/3, we transiently transfected cells with ScarWA, the COOH-terminal part of Scar1, which binds to Arp2/3 and whose overexpression into cells leads to the sequestration of the Arp2/3 complex (Machesky and Insall, 1998). In cells transiently transfected with ScarWA, the formation of InlB-mediated ruffles decreased by 95 ± 1%, whereas transfection with ScarW, a fragment that does not bind Arp2/3, had no effect on InlB-induced ruffling (Fig. 2 B). These results are consistent with a role of the Arp2/3 complex in the formation of InlB-mediated membrane ruffles, even though we cannot rule out an indirect inhibitory effect of ScarWA in disrupting the actin cytoskeleton.

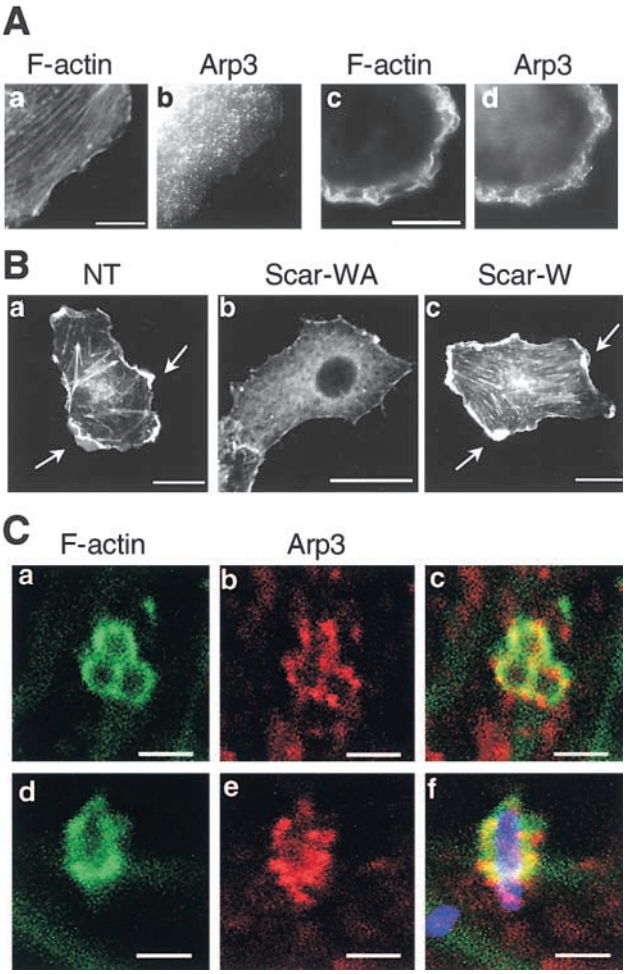

Figure 2. **A role for the Arp2/3 complex in InlB-induced membrane ruffles and phagocytosis.** (A) Recruitment of the Arp2/3 complex to InlB-induced ruffles. Vero cells, untreated (a and b) or stimulated with 4.5 nM of InlB (c and d) stained with FITC-phalloidin and anti-Arp3 Ab. (B) Inhibition of InlB-induced ruffles in ScarWA-transfected cells. Vero cells, nontransfected (NT, a) or transiently transfected with ScarWA (b) or ScarW (c) stimulated with InlB and stained with FITC-phalloidin. (C) Recruitment of the Arp2/3 complex to InlB beads (a–c) or bacteria- (d–f) induced phagocytic cups. Cells were stained with FITC-phalloidin (green) and anti-Arp3 Ab (red). The bacterium is labeled with anti-InlA Ab (f, blue). Images represent confocal slices of 0.6 (beads) and 1.2 μm (bacteria). Bars: (A) 10 μm; (B) 20 μm; (C) 2 μm.

To investigate a role of the Arp2/3 complex in InlB-mediated entry, we first examined the recruitment of the Arp2/3 complex beneath InlB particles when F-actin cups are maximally formed (10 min for beads and 20 min for bacteria). Experiments were performed in Vero cells and also in Ref52 cells, a fibroblast cell line permissive for InlB-mediated entry but in which, interestingly, InlB stimulation does not lead to membrane ruffle formation. In both Vero (Fig. 2 C) and Ref52 cells (unpublished data), Arp3 colocalized with F-actin cups around entering beads or bacteria. No labeling was observed around extracellular or intracellular particles that were not associated with F-actin. We quantified entry of InlB beads into ScarWA or ScarW-expressing cells. Bead en-

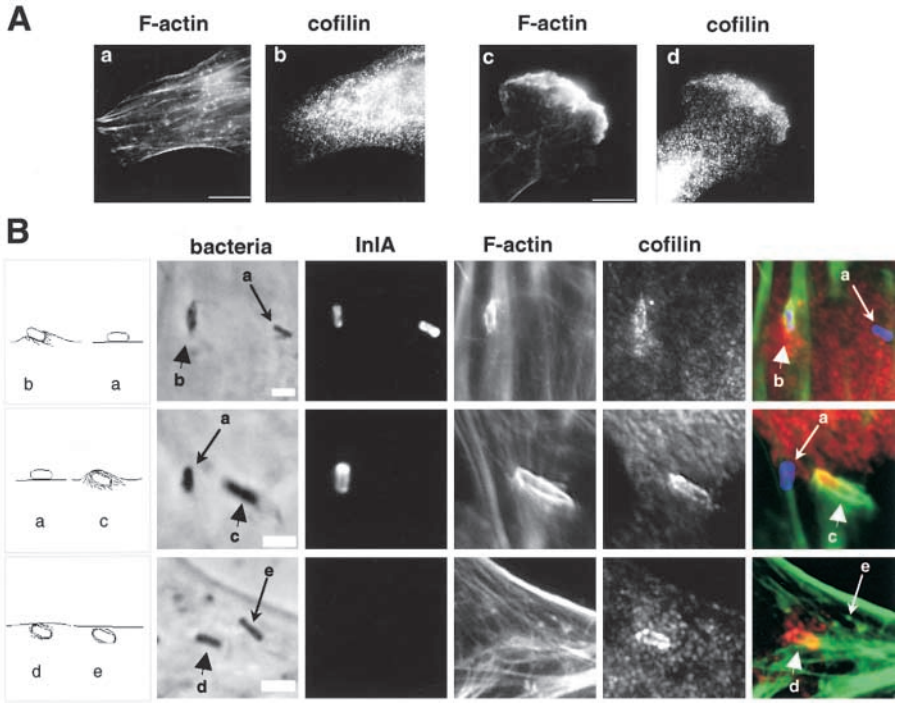

Figure 3. **Cofilin is recruited to InlB-induced membrane ruffles and phagocytic cups.** (A) Colocalization of cofilin with F-actin in InlB-induced ruffles. Vero cells, untreated (a and b) or stimulated with 4.5 nM of InlB (c and d) stained with FITC-phalloidin and anti-cofilin Ab. (B) Recruitment of cofilin by bacteria at different stages of the internalization process in Ref52 cells. The left panels schematically represent the bacteria detected in the five other panels and marked by reference to Fig. 1 A. Total bacteria associated with cells was visualized in phase–contrast, and bacteria that are fully or partly extracellular were identified by labeling with anti-InlA Ab before cell permeabilization. Cells were stained with FITC-phalloidin and anti-cofilin Ab. In the merged images, extracellular bacteria are blue, F-actin is green, and cofilin is red. Arrowheads or arrows indicate bacteria that colocalizes or not with cofilin, respectively. Bars: (A, a) 10 μm; (A, c) 2 μm.

try was inhibited by 77 ± 5% and 56 ± 6% into ScarWA-expressing Vero or Ref52 cells, respectively, compared with that into nontransfected cells. In contrast, expression of ScarW or transfection of a pEGFP control plasmid had no effect on internalization. Thus, these results strongly suggest that recruitment of the Arp2/3 complex is required in the InlB-mediated internalization process.

Cofilin is recruited to InlB-induced ruffles and during InlB-mediated entry

ADF/cofilin has been localized in lamellipodia (Svitkina and Borisy, 1999; Chan et al., 2000) and in phagocytic cups (Aizawa et al., 1997; Nagaishi et al., 1999). Therefore, we investigated whether it was recruited in InlB-induced ruffles and during the InlB-mediated entry process. Experiments on entry were performed only with bacteria, since our anti-cofilin antibodies reacted with the beads used in immunofluorescence studies. As for Arp2/3, cofilin was localized in InlB-induced actin-rich membrane ruffles (Fig. 3 A) and with bacterial phagocytic cups (see below). Interestingly, resting Ref52 cells displayed a more intense cytoplasmic cofilin staining than Vero cells and therefore were chosen for analyzing in detail the spatial distribution of cofilin during InlB-induced entry. Cofilin was not detected underneath extracellular bacteria that were only adherent (Fig. 3 B, bacteria a) but colocalized with F-actin rings around bacteria being internalized (Fig. 3 B, bacteria b and c). Strikingly, the most intense cofilin labeling was observed around some of the newly internalized intracellular bacteria, poorly labeled by FITC-phalloidin (Fig. 3 B, bacterium d). This observation may reflect the fact that phalloidin fails to bind to actin filaments saturated with cofilin (Chen et al., 2000). At the same time point (20 min after infection), other intracellular bacteria were no longer associated with cofilin and F-actin (Fig. 3 B, bacterium e). Taken together, these results suggested that cofilin may accumulate progressively and transiently at the InlB-induced phagosome and then induce rapid actin depolymerization. Thus, cofilin would be involved in both assembly and disassembly of the InlB-induced phagocytic cup.

Modulation of LIMK activity affects *L. monocytogenes* actin-based motility in vivo

Overexpressing LIMK1 into cells is known to increase cofilin phosphorylation thereby inactivating cofilin. Conversely, overexpression of LIMK1$^-$, a kinase-dead variant that has a dominant negative effect on endogenous LIMK, reduces cofilin phosphorylation thereby activating cofilin and inhibiting F-actin accumulation (Arber et al., 1998; Yang et al., 1998). To investigate the function of cofilin in InlB-mediated cytoskeleton rearrangements, we used these LIMK constructs as a mean of modulating endogenous cofilin's activity in vivo. As expected, expression of LIMK1 in Vero cells induced prominent F-actin stress fibers in agreement with an inhibition of actin depolymerization upon cofilin phosphorylation, whereas expressing LIMK1$^-$ slightly reduced the F-actin (FITC-phalloidin) staining (Fig. 4 A). Then, we verified that expression of these constructs could affect a process known to require cofilin's activity, the *Listeria*-actin–based motility. After escape from the phagocytic vacuole, *Listeria* polymerizes actin and forms comet tail structures, which promote bacterial movement within the cytosol. Actin turnover in tails of bacteria moving in cell extracts is cofilin dependent (Carlier et al., 1997; Rosenblatt et al., 1997; Loisel et al., 1999). We analyzed formation of *Listeria* actin tails in LIMK1- and LIMK1$^-$-expressing Vero cells. In LIMK1-transfected cells, some bacteria exhibited unusual long comet tails (Fig. 4 B), and the mean tail length increased to 15.3 ± 5.8 μm compared with 6.1 ± 1.8 μm in the neighboring nontransfected cells. The efficiency of tail formation (see Materials and methods) also increased by 90% relative to that in nontransfected cells. Interestingly, LIMK1 was lo-

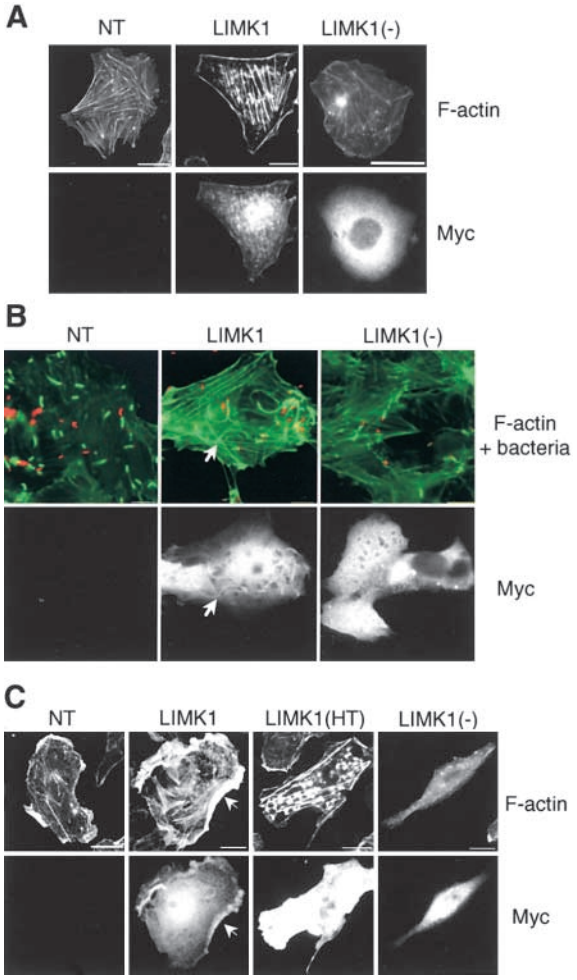

Figure 4. **LIMK1 and LIMK1$^-$ expression affect *Listeria* actin-based motility and InlB-mediated ruffling.** Vero cells nontransfected (NT) or transiently transfected with LIMK1 or LIMK1$^-$ stained with FITC-phalloidin and with anti-Myc Ab to detect the LIMK1 and LIMK1$^-$ fusion proteins. (A) Resting cells. (B) Cells infected with the *Listeria* variant EGDΔ*inlB*(LRRs-IR-SPA) and analyzed for actin tail formation. F-actin is in green and bacteria are in red. LIMK1 accumulates in long comet tails (arrows). (C) Cells stimulated with 4.5 nM of InlB for 5 min and analyzed for membrane ruffle formation. LIMK1 accumulates in the ruffle areas (arrows). LIMK1(−), LIMK1(−); LIMK1(HT), LIMK1 highly transfected cells. Bars: (A) 20 μm; (B) 10 μm; (C) 20 μm.

calized in the tails, suggesting that it was actively recruited there. In LIMK1$^-$-transfected cells, bacteria still induced actin polymerization at the bacterial surface (Fig. 4 B), but the efficiency of tail formation decreased by 65%, and the tail length was slightly decreased to 3.9 ± 0.9 μm versus 6.6 ± 0.6 μm in the nontransfected cells. These results are consistent with previous experiments using immunodepletion or addition of cofilin in vitro (Rosenblatt et al., 1997) and strongly suggest that LIMK1 or LIMK1$^-$ expression modulates cofilin's activity inside Vero cells.

A role for cofilin and LIMK in InlB-mediated membrane ruffling and entry

We analyzed the effects of LIMK1 and LIMK1$^-$ expression on the formation of InlB-induced ruffles and phagocytosis. When stimulated with InlB, LIMK1-expressing cells were positive for ruffling, as were nontransfected cells, but displayed larger membrane ruffles enriched in F-actin (Fig. 4 C). In contrast, in cells expressing very high levels of LIMK1 (LIMK1 HT, ∼10% of the transfected cells; see Materials and methods) the formation of InlB-mediated ruffles decreased by 80%. It is possible that in those cells the whole cofilin pool is inactivated by phosphorylation, resulting in full inhibition of the ruffling process as shown recently for EGF-induced lamellipod extension (Zebda et al., 2000). Moreover, since F-actin aggregates appeared in these cells (Fig. 4 C), some actin regulatory proteins may have been sequestered and no longer available for membrane ruffle formation. These cells were not taken into account in the other quantification experiments. Expression of the dominant negative LIMK1$^-$ prevented the formation of InlB-mediated ruffles (Fig. 4 C) by 35 ± 7% compared with nontransfected cells as observed previously for other agonists such as insulin (Yang et al., 1998). Since cofilin (Fig. 3 A) and the overexpressed LIMK1 (Fig. 4 C) were localized in ruffles, these proteins are likely to be involved in the InlB-mediated ruffling process.

InlB bead entry was also quantified into Vero or Ref52 cells expressing LIMK1 or LIMK1$^-$. 10 min after infection, the number of beads associated with F-actin rings in LIMK1-expressing cells was not statistically different from that in the surrounding nontransfected cells. Yet, 40 min after infection when the internalization process is fully achieved in the nontransfected cells (Fig. 1 B) entry of InlB beads into cells expressing LIMK1 was decreased significantly by 34 ± 3% in Vero cells and by 35 ± 6% in Ref52 cells compared with the efficiency of entry into the nontransfected cells. Quite strikingly, in these cells F-actin rings were abnormal, most often thicker and enriched in F-actin and/or with irregular shapes, consistent with an uncontrolled actin depolymerization process (Fig. 5 A). Such a phenomenon also occurred when LIMK1-expressing cells were infected with bacteria, with the appearance of large F-actin foci beneath entering bacteria (Fig. 5 B). In addition, LIMK1 colocalized with F-actin around InlB beads or bacteria, suggesting that it is actively recruited at the entry site. These results suggested that LIMK1 overexpression inhibits particle engulfment into the cell and phagocytic cup closure.

Bead uptake into cells transiently transfected with the dominant negative LIMK1$^-$ also decreased 40 min after infection by 46 ± 8% in Vero cells and 61 ± 7% in Ref52 cells. However, inhibition was not linked to a modification of the actin cup shape (Fig. 5) but to an inhibition of the actin cup formation. The number of InlB beads associated with F-actin rings 10 min after infection consistently decreased (18.8 ± 1.5% in LIMK1$^-$ versus 55.1 ± 1.4% in nontransfected Vero cells in two independent experiments), indicative of a global downregulation of the entry process. Taken together, these results strongly suggested that the cofilin phosphocycle plays a critical role in InlB-mediated internalization.

Expression of the nonphosphorylatable S3A cofilin mutant prevents InlB-induced ruffling and phagocytosis and decreases comet tails length

The inhibition of InlB-mediated entry and ruffling and that of comet tails formation in LIMK1$^-$-expressing cells suggested

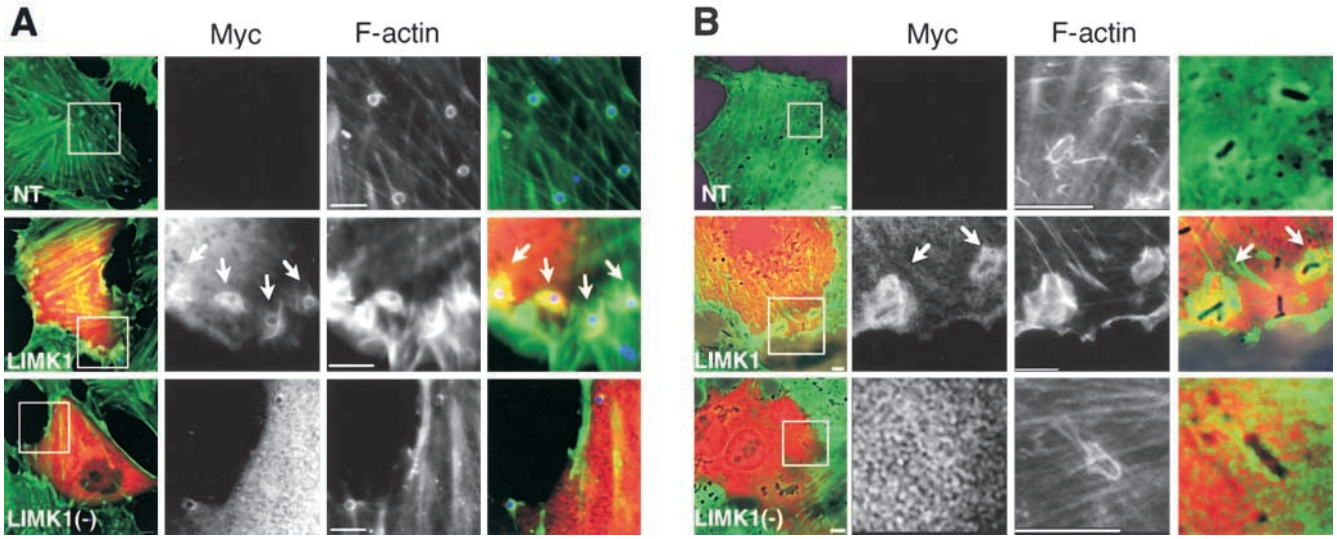

Figure 5. **Effects of LIMK1 and LIMK1⁻ expression on the formation of F-actin cups at the entry site of InlB beads and bacteria.** Vero cells nontransfected (NT) or transiently transfected with LIMK1 or LIMK1⁻ incubated with InlB beads for 10 min (A) or with bacteria for 20 min (B) stained with anti-Myc Ab to detect the LIMK1 and LIMK1⁻ fusion proteins and FITC-phalloidin. Boxed regions in the left panels indicate the position of the field, which is magnified in the images on the right panels. In the merged images, total InlB beads are blue, F-actin is green, Myc is red, and the bacteria are visualized in phase–contrast. LIMK1 colocalized with F-actin in abnormal phagocytic cups (arrows). Bars, 5 μm.

Figure 6. **S3A cofilin recruitment to InlB-induced ruffles, InlB-mediated phagocytic cups, and *Listeria* comet tails decreases the amount of F-actin in these structures.** Vero cells transiently transfected with S3A cofilin were left unstimulated (resting cells) or analyzed for the formation of InlB-induced ruffles, phagocytic cups, or *Listeria* comet tails as described in the legends to Figs. 4 and 5. Cells were stained with FITC-phalloidin, anti-Myc Ab to detect S3 cofilin, and for comet analysis with anti-*Listeria* Ab. In the merged images, F-actin is green, S3A cofilin is red, and InlB beads or bacteria are blue. S3A cofilin is localized in reduced membrane ruffles (magnified in boxed regions), thin phagocytic cups, and short comet tails (arrows). Arrowheads indicate cofilin rods (rd). Bar: (first and second rows) 10 μm; (boxed images and third and fourth rows) 2 μm.

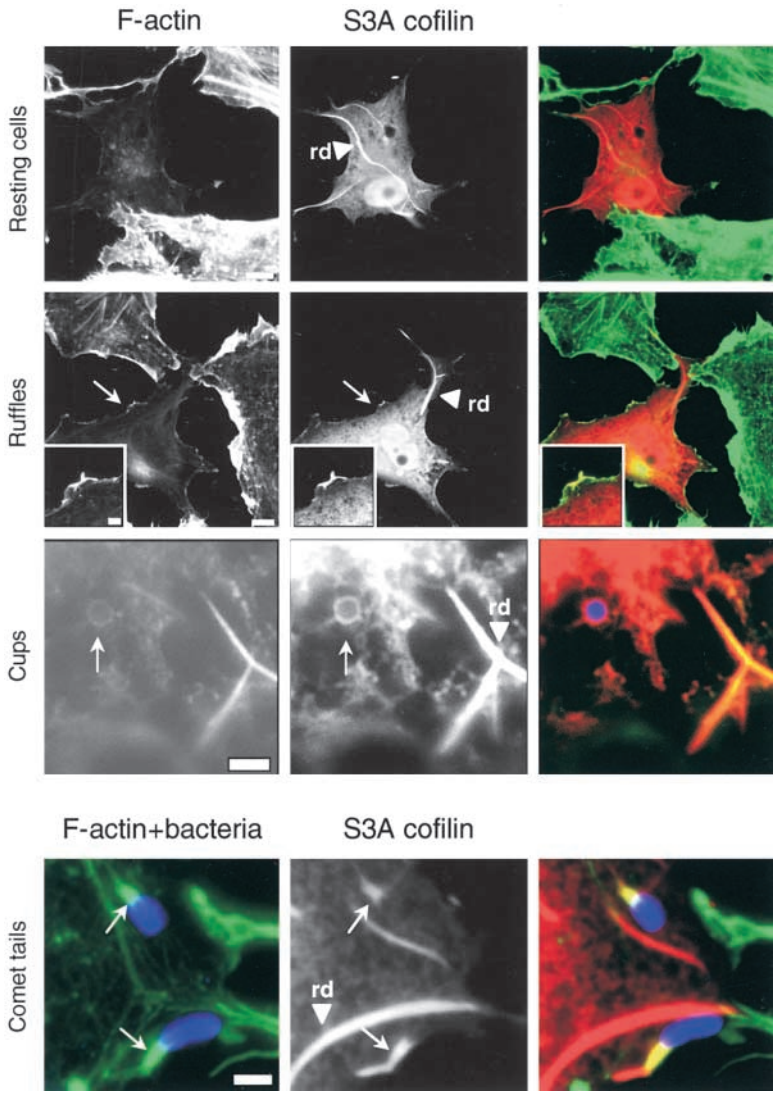

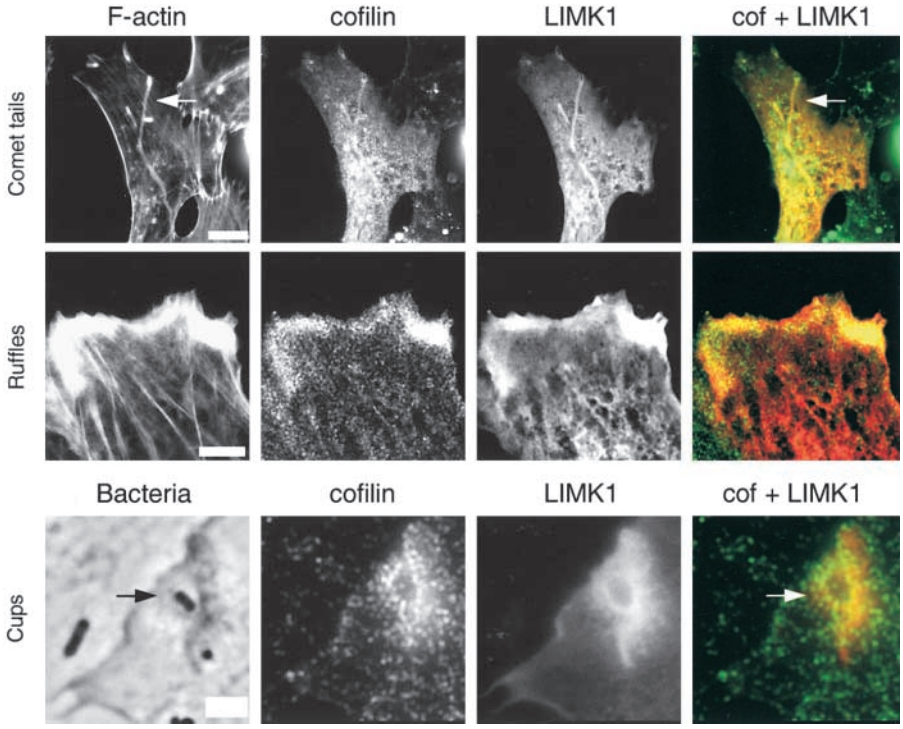

Figure 7. **In LIMK1-overexpressing cells, endogenous cofilin is still recruited to actin-based structures.** Vero cells transiently transfected with LIMK1 were analyzed for *Listeria* tail formation, InlB-induced ruffling, or bacterial entry as described in the legends to Figs. 4 and 5. Cells were stained with FITC-phalloidin, anti-Myc, and anti-cofilin Ab. In the merged images, cofilin is green and LIMK1 is red. Bars: (first and second rows) 10 μm; (third row) 2 μm.

that phosphorylation and thus inactivation of cofilin by endogenous LIMK is critical to these three types of actin-based processes. To address this issue by an alternative approach, we analyzed the effects of increasing cofilin's activity into cells by overexpressing cofilin (wt cofilin) or a nonphosphorylatable and constitutively active mutant (S3A cofilin). The S3A cofilin mutant lacks the physiological phosphorylation site on serine 3 and therefore cannot be inactivated by endogenous LIMK. As shown previously in other cell types (Arber et al., 1998), expression of these cofilin constructs into Vero cells led to the formation of typical cofilin rods and pronounced loss of actin filament structure in comparison with the neighboring nontransfected cells (Fig. 6, first row; unpublished data). These phenomenons were more pronounced in S3A-expressing cells (80% of S3A versus 50% of wt cofilin–positive cells exhibited rods), consistent with an increased cofilin activity. When stimulated with purified InlB, S3A-expressing cells were positive for ruffling as were the nontransfected cells or wt cofilin–transfected cells, but the area of ruffling and the F-actin content in these structures was reduced dramatically (Fig. 6, second row). In the same way, the F-actin staining at phagocytic cups during InlB bead internalization was less intense in S3A-expressing cells than in the nontransfected cells (Fig. 6, third row, compared with Fig. 5 A, first row). Moreover, InlB bead entry was decreased by 48 ± 5% into S3A-expressing cells compared with that into the neighboring cells. In contrast, the efficiency of InlB bead uptake into wt cofilin–expressing cells was not significantly different from that into the nontransfected cells. Lastly, concerning the intracellular motility of *Listeria*, the mean comet tail length in S3A-positive cells was strongly decreased (1.6 ± 0.9 μm versus 5.6 ± 3.8 μm in the neighboring nontransfected cells; Fig. 6, fourth row), whereas tail lengths in wt cofilin–positive cells were only slightly decreased (3.6 ± 2.1 μm versus 4.3 ± 2.7 μm in the nontransfected cells). Like endogenous cofilin, S3A and wt cofilin colocalized with membrane ruffles, actin cups, and tails (Fig. 6; unpublished data). Therefore, these data provide evidence that expressing an active nonphosphorylatable cofilin mutant affects cytoskeletal rearrangements in a way highly reminiscent of that observed upon inhibition of LIMK activity.

Overexpression of S3A cofilin suppresses accumulation of F-actin induced by LIMK1 overexpression

We next determined whether the accumulation of actin filaments observed upon overexpression of LIMK1 may be related directly to the local phosphorylation and deactivation of cofilin. In LIMK1-expressing cells, endogenous cofilin was still localized in F-actin–rich tails, ruffles, and phagocytic cups, indicating that LIMK1 expression did not prevent cofilin recruitment into these structures (Fig. 7). To correlate the formation of these prominent actin structures to phosphorylation of cofilin, we carried out cotransfection experiments with LIMK1 together with the nonphosphorylatable S3A cofilin in Vero cells. As expected, coexpression of S3A with LIMK1 suppressed any detectable effect of LIMK1 overexpression on the actin cytoskeleton, preventing F-actin accumulation into comet tails, ruffles, and phagocytic cups (Fig. 8 compared with Figs. 4 and 5). Amazingly, in these coexpressing cells the LIMK1 anti-tag antibody did not label cofilin rods (Fig. 8). It did not label either comet tails (Fig. 8) or bacterial-induced phagocytic cups (unpublished data), in contrast to what happened in cells expressing only LIMK1 (Fig. 7). This lack of colocalization may indicate that LIMK1 does not bind S3A cofilin or results from a more complex phenomenon. Taken together, these data provide evidence that induced F-actin accumulation and stabilization of actin filaments at phagocytic

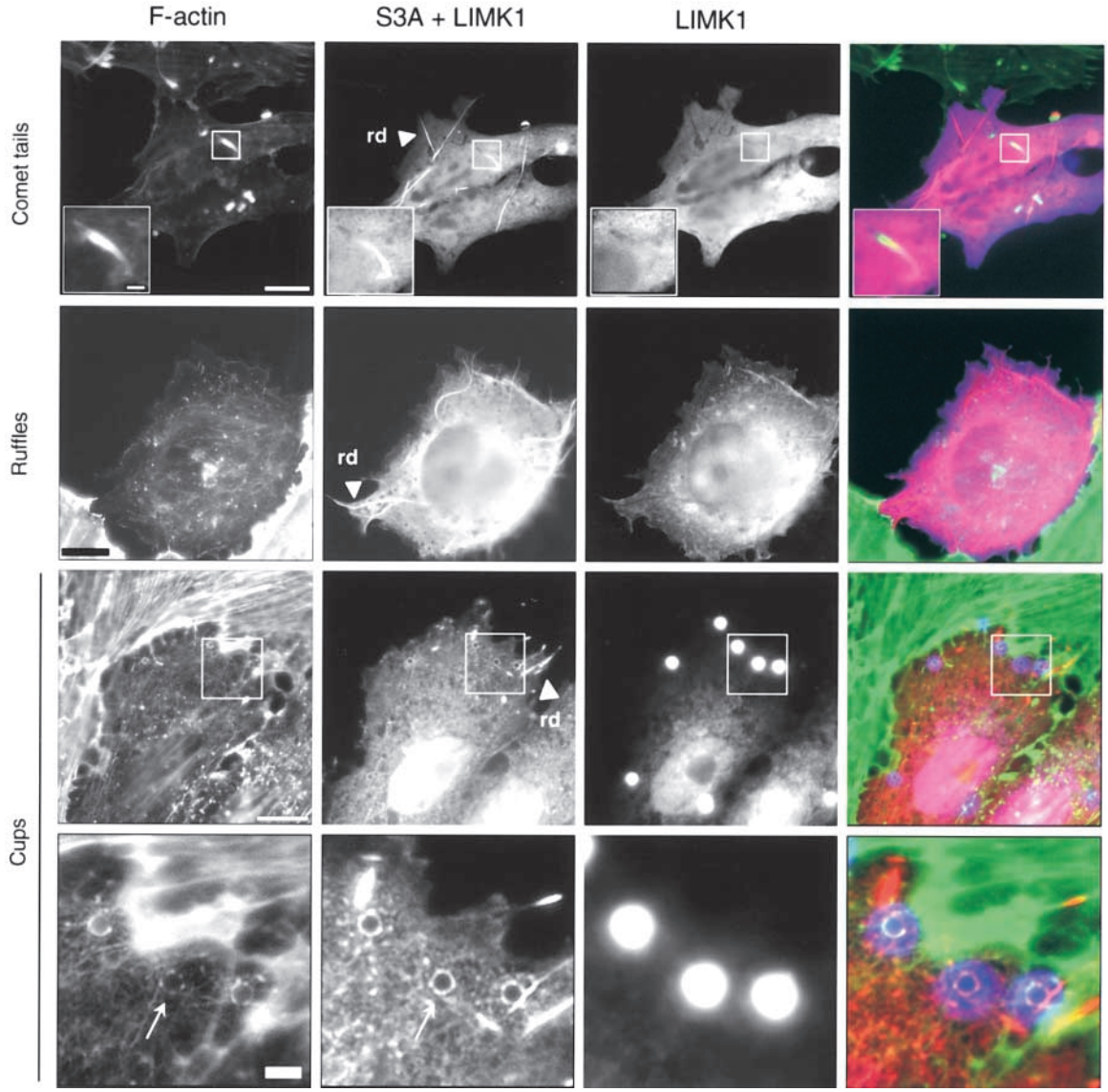

Figure 8. **Overexpression of S3A cofilin suppresses F-actin accumulation induced by LIMK1 overexpression.** Vero cells transiently cotransfected with LIMK1 and S3A cofilin cDNAs were analyzed for formation of *Listeria* tails, InlB-induced ruffles, or InlB bead phagocytic cups as described in the legends to Figs. 4 and 5. Cells were stained with FITC-phalloidin, anti-Myc, which detects both LIMK1 and S3A fusion proteins and lights up cofilin rods (arrowheads, rd), and an antipeptide Ab specific only to the LIMK1 fusion protein. For cups, boxed regions indicate the position of the field, which is magnified below. Due to their intrinsic fluorescence in the 650–700-nM range, InlB beads are detected together with the Cy5-labeled LIMK1 anti-tag. In the merged images, F-actin is green, Myc is red, and LIMK1 and InlB beads are blue. Bars: (full images) 10 μm; (magnified images) 2 μm.

cups, ruffles, and comet tails into LIMK1-expressing cells occurs through phosphorylation and inhibition of cofilin.

A role for Rac in InlB-mediated cytoskeleton rearrangements

LIMK1 is a downstream effector of Rac and is involved in Rac-induced lamellipodium formation (Yang et al., 1998). To examine the role of Rac and other GTPases in InlB-mediated cytoskeletal rearrangements, we quantified ruffle formation in InlB-stimulated Vero cells transiently transfected with rac1-N17, cdc42-N17, and rhoA-N19 dominant negative constructs. Expression of rac1-N17 and cdc42-N17 inhibited InlB-induced membrane ruffling by 98 ± 2% and 60 ± 3%, respectively, whereas rhoA-N19 had no effect on that process. Then, we examined the role of these Rho GTPases on InlB-mediated internalization in Vero and Ref52 cells. Expression of rac1-N17 and cdc42-N17 but not rhoA-N19 clearly inhibited InlB bead entry in Ref52 cells (by 59 ± 5% and 47 ± 5%, respectively). Surprisingly, only rac1-N17 inhibited entry in Vero cells (by 58 ± 4%), whereas cdc42-N17 and rhoA-N19 mutants had no effect on entry in this cell line. The relative importance of Cdc42 in InlB-induced phagocytosis may be linked to variations in cell sensitivity to the dominant negative construct and/or to the bypass of the Cdc42 pathway. A possible role of RhoA in InlB-induced phagocytosis cannot yet be excluded. Taken together, our results indicate that InlB-mediated cytoskeletal rearrangements depend on the activity of Rac.

Discussion

In this work, we analyzed temporally and spatially the actin rearrangements that take place during InlB-induced phagocytosis of *L. monocytogenes*. We identified the Arp2/3 complex, Rac, LIMK, and ADF/cofilin as key proteins in this phenomenon. Moreover, we report that the tight phosphoregulation of cofilin's activity during the transient and successive actin polymerization and depolymerization steps is crucial for an efficient phagocytic process.

Entry of InlB-coated particles occurs within minutes. Concomitantly, InlB particles are surrounded by F-actin in a very transient fashion, revealing a two-phase process of rapid actin polymerization and depolymerization events. Interestingly, the rate of entry and actin recruitment is faster in the case of beads than for bacteria, although the overall efficiency of entry after 1 h of infection is the same. Since the size of both types of particles is approximately the same (1 μm), this result may indicate that bacterial factors other than InlB are involved in a regulatory step of the entry process. In line with this hypothesis, the listerial factor LLO modulates the rate of *Listeria* uptake by macrophages (Wadsworth and Goldfine, 1999).

Soluble InlB elicits membrane ruffles, whereas entry of invasive InlB beads or bacteria is not associated with this type of morphological changes. Here, we show that both phenomenons involve the same regulatory proteins. The Arp2/3 complex colocalizes with F-actin in InlB-mediated ruffles and around entering InlB-coated beads or bacteria, and both InlB-mediated ruffles and internalization are inhibited in cells expressing ScarWA, the COOH-terminal part of Scar1 known as an inhibitor of Arp2/3 recruitment in vivo (Machesky and Insall, 1998). These results are in agreement with the requirement of the Arp2/3 complex in growth factor-mediated lamellipodia and ruffle formation (Machesky and Insall, 1998; Bailly et al., 1999) and in FcγR and CR3-mediated phagocytosis (May et al., 2000). The Arp2/3 complex is also localized with F-actin during cytoskeletal rearrangements mediated by enteropathogenic *Escherichia coli* (Kalman et al., 1999), *Salmonella* (Stender et al., 2000), or *Borrelia* (Linder et al., 2001) and appears as a general inducer of the actin polymerization triggered by a variety of pathogens.

Cofilin is involved in *Listeria* actin-based motility (Rosenblatt et al., 1997; Loisel et al., 1999) and lamellipodia extension (Svitkina and Borisy, 1999; Chan et al., 2000). In addition, cofilin has been localized with phagosomes in *Dictyostelium* (Aizawa et al., 1997), and microinjection of anticofilin antibodies inhibits phagocytosis of opsonized zymosan in neutrophils (Nagaishi et al., 1999). Here, we show that cofilin is recruited at InlB-induced phagocytic cups and that both down- and upregulation of cofilin's activity inhibits InlB-induced internalization. Thus, the cofilin phosphocycle is critical for efficient phagocytosis.

Overexpressing LIMK1 induces a dramatic change in the shape and thickness of the F-actin cup at the entry site of InlB particles, often with appearance of large and abnormal actin foci beneath particles, leading to a decrease in entry. In agreement with previous studies (Rosenblatt et al., 1997; Arber et al., 1998; Yang et al., 1998; Edwards et al., 1999), we also report that overexpressing LIMK1 greatly lengthens and increases the number of actin comet tails during *Listeria* intracellular movement and the extent of InlB-induced ruffles. All of these observations are consistent with a reduction of the F-actin depolymerization process and actin turnover as a result of local inactivation of cofilin as shown previously for the rate of *Listeria* movement (Carlier et al., 1997) and the rate of formation of membrane ruffles (Arber et al., 1998). Expression of a nonphosphorylatable S3A cofilin mutant suppresses all the phenotypes resulting from LIMK1 overexpression, indicating that the observed effects are linked to cofilin phosphorylation. Interestingly, expressing LIMK1 does not lead to the full inhibition of actin-based processes, whereas expression of the kinase domain of LIMK1 (K1) alone completely inhibits EGF-induced lamellipod formation (Zebda et al., 2000). This discrepancy may be due to a weaker and differential inhibition of cofilin's activity upon LIMK1 rather than K1 overexpression. A moderate overexpression of LIMK1 may inactivate only the depolymerizing activity of cofilin, leading to the slow-down of actin dynamics, whereas overexpressing the K1 fragment may inactivate mainly severing activity, leading to complete inhibition of actin dynamics (Chan et al., 2000; Zebda et al., 2000). Our data also show that hyperactivation of cofilin by inhibiting endogenous LIMK or by expressing S3A cofilin alone reduces *Listeria* tail length and impairs InlB-induced ruffles and phagocytosis. In S3A-positive cells, phagocytic cups exhibit low F-actin content. In cells expressing LIMK1^{-}, the number of entering particles associated with F-actin cups decreases, suggesting that inhibition of LIMK blocks the initial actin polymerization step. Therefore, both overexpression and inhibition of LIMK affect tail formation, ruffling, and phagocytosis, consistent with the fact that tight control of the local concentration of active cofilin is crucial for these actin-dependent processes. LIMK1 colocalizes with F-actin in comet tails, membrane ruffles, and the phagocytic cups, which reinforces the idea that it is involved in the formation of these dynamic structures.

What would be the role of cofilin and its phosphocycle in the entry process? Cofilin is recruited at the InlB-induced phagocytic cup, and its concentration seems to progressively increase, since the cofilin labeling is more intense around the newly formed phagosomes than around unclosed phagocytic cups. This observation suggests cofilin may regulate two steps of the entry process (Fig. 9 A). At low concentration, cofilin could be involved in the phagocytic cup extension by stimulating actin dynamics. At this step, LIMK could be recruited to inactivate excess amounts of cofilin on elongating filaments. Then, the progressive accumulation of cofilin on the filaments would ultimately favor the disassembly of the actin network during the retraction of the phagocytic cup and around the newly formed phagosome. In line with this scenario, increasing the pool of active cofilin by expressing the constitutively active S3A cofilin or by inhibiting endogenous LIMK blocks the phagocytic cup formation, presumably due to an excess of depolymerizing activity (Fig. 9 B). Conversely, partial inactivation of cofilin by overexpressing LIMK1 induces an intense and disorganized accumulation of actin filaments at the phagocytic cup, preventing the engulfment of the particle into the cell and resulting in inhibi-

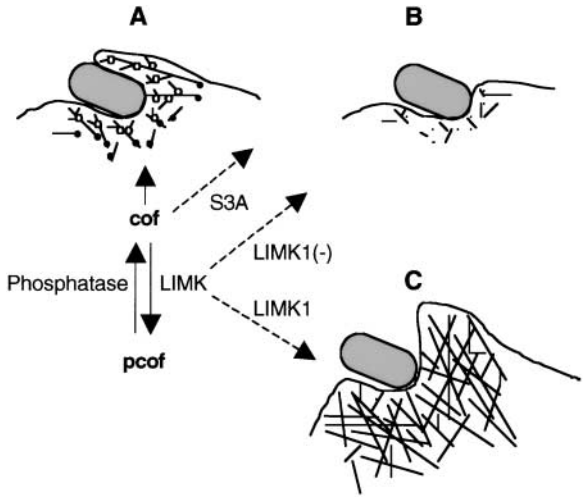

Figure 9. **Possible role of the cofilin phosphocycle in InlB-induced phagocytosis.** (A) Interaction of InlB with its receptors triggers actin polymerization and formation of the phagocytic cup. This step involves recruitment of (1) the Arp2/3 complex (open circles), which promotes actin nucleation and branching of the filaments, and (2) ADF/cofilin (closed circles), which stimulates actin dynamics by severing actin filaments, creating new ends that allow actin polymerization, and by depolymerizing actin filaments, supplying new actin monomers. LIMK recruited at this step could prevent excessive depolymerization of the filaments by partly inactivating cofilin. A phosphatase could reactivate cofilin, which would finally accumulate on the filaments, thereby increasing its activity and facilitating the disruption of the F-actin network in the phagocytic cup. (B) Inhibition of endogenous LIMK by expressing the dominant negative LIMK1$^-$ or expression of the nonphophorylatable S3A mutant would lead to an excessive activity of cofilin, resulting in increased filament disassembly and abortion of the actin cup formation. (C) Overexpressing LIMK1 would increase cofilin phosphorylation, leading to the inhibition of its actin depolymerizing activity and inducing the formation of a rigid structure beneath the entering particles made of a thick filament network. These events would prevent the engulfment of the particle into the cell, resulting in the inhibition of the phagocytic cup closure.

tion of the phagocytic cup closure (Fig. 9 C). In this model, alteration of cofilin's activity disturbs the coordinated action of two opposite forces, one which triggers the phagocytic cup extension and the other which is required to pull the particle into the cell. Future work will be required to validate this model at the molecular level and to dissect the contribution of other regulatory molecules.

Taken together, our results indicate for the first time that the Arp2/3 complex, ADF/cofilin, and LIMK are effectors of Met-induced signals to the cytoskeleton. As we have shown here, InlB-mediated membrane ruffles and phagocytosis are dependent on Rac, consistent with the previous findings on the role of this GTPase in HGF/Met-dependent actin reorganization (Ridley et al., 1995). HGF/Met were also shown to activate Rac and the p21-activated kinase PAK (Royal et al., 2000). Since PAK activates LIMK in another system (Edwards et al., 1999), our results strongly suggest that InlB–Met interactions elicits a Rac→ PAK → LIMK → cofilin-signaling cascade.

In conclusion, we have identified cofilin as a novel regulatory component in bacterial-induced phagocytosis. Interestingly, other invasive bacteria also modulate their uptake into cells by controlling the reversal of actin rearrangements. *Shigella* and *Salmonella* enter into epithelial cells by a "trigger" mechanism achieved by delivery of bacterial proteins into the host cytosol and associated with the formation of cellular projections and cytoskeleton reorganization. Some of these proteins are dedicated to trigger actin polymerization. Others like the *Shigella* IpaA protein induce depolymerization of actin filaments (Bourdet-Sicard et al., 1999). An IpaA mutant displays disorganized protrusions at the entry site and is defective in entry (Tran Van Nhieu et al., 1997). This phenomenon presents similarities with the uncontrolled actin polymerization at the InlB phagocytic cup in cells in which cofilin's activity is inhibited. Therefore, cofilin or the IpaA–vinculin complex both facilitate bacterial entry by promoting filament disassembly at *Listeria* actin cups or *Shigella* actin foci, respectively. In *Salmonella*, the protein SptP modulates entry by acting as a GTPase-activating protein for Rac1 and Cdc42, resulting in the downregulation of the signals inducing actin cytoskeleton rearrangements (Fu and Galan, 1999). All of these findings indicate that invasive bacteria have evolved strategies to tightly modulate their uptake by eukaryotic cells, not only by inducing actin polymerization necessary for this process but also by downregulating it.

Materials and methods

Bacteria, cells, and reagents

The *L. monocytogenes* variant EGDΔ*inlB*(LRRs-IR-SPA) was obtained by electroporating plasmid pPIB8 into stain EGDΔ*inlB* (Braun et al., 1999) and grown at 37°C in brain-heart infusion agar (Difco). Vero and Ref52 cells were cultured in DME (GIBCO BRL) supplemented with 10% FCS (Sera-Lab), 2 mM glutamine, and 1% nonessential amino acids at 37°C in 10% CO_2. Covalent coupling of purified InlB protein to latex beads (F8817; Molecular Probes) was performed as described (Braun et al., 1998).

Transient transfections

Vero or Ref52 cells (2.5×10^4/ml) were plated on coverslips, transfected 18 h later using lipofectamine-plus (GIBCO BRL) and used in invasion, ruffling, or *Listeria* motility assays 24 h after transfection. The plasmids used were pEGFP-C1 (CLONETECH Laboratories, Inc.), pRK5-Myc derivatives, encoding ScarWA, ScarW (Machesky and Insall, 1998), rac1-N17, cdc42-N17, or rho-N19 (a gift from A. Hall, University College, London, UK), and pcDNA3 (Invitrogen) derivatives encoding LIMK1, LIMK1$^-$, rat cofilin (wt), and its nonphosphorylatable S3A mutant (Arber et al., 1998). High-expressing LIMK1 cells were distinguished from moderate expressors by saturation of fluorescence of the Myc staining after 0.02 s of exposure time. These cells always contained actin clumps. Cells cotransfected with LIMK1 and S3A cofilin at a ratio of 1:2 were selected by staining with anti-GLVVMNIT, which detects LIMK1 expression, and with anti-Myc, which detects both LIMK1 and S3A cofilin expression and lights up cofilin rods.

Invasion assays and immunofluorescence analysis

Vero or Ref52 cells (5×10^4/ml) were seeded onto coverslips in 24-well plates and grown for 48 h or were transfected as described above. To synchronize entry, cells were washed in DME, kept at 4°C for 20 min, and incubated with washed InlB-coated particles at a multiplicity of infection of 5–10 per mammalian cells with centrifugation at 200 *g* for 1 min at 4°C. After a wash in DME, internalization was started by warming at 37°C in 10% CO_2. To stop internalization, cells were washed once with ice-cold PBS and fixed in ice-cold 3% paraformaldehyde (PFA)/PBS. The mixture was immediately replaced by fresh PFA, and fixation continued for 20 min at room temperature. When indicated, extracellular particles were labeled with the indicated antibodies. Cells were then permeabilized for 4 min with 0.4% Triton X-100 in CSK buffer as described (Diakonova et al., 1995), washed in CSK and PBS, and stained for the indicated antibodies. The primary antibodies used were polyclonal antibodies raised against *L. monocytogenes* (R11; Gouin et al., 1995), InlB (Braun et al., 1997), h-Met (C-28; Santa Cruz Biotechnology, Inc.), Arp3 and cofilin (David et al.,

1998), and GLVVMNIT (Arber et al., 1998), and monoclonal antibodies raised against Myc (9E10; SC), InlB (B4-6; Braun et al., 1999), and InlA (L7-7; Mengaud et al., 1996b). The secondary antibodies used were FITC-conjugated (Biosys), Cy3-conjugated, Cy5-conjugated (Jackson ImmnuoResearch Laboratories), or Alexa 546– or Alexa 488–conjugated (Molecular Probes) goat anti–mouse or anti–rabbit IgGs antibodies. Total bacteria were visualized in phase–contrast, and total InlB beads were detected by their intrinsic fluorescence in the 650–700 nM range. F-actin was labeled with FITC-phalloidin. Preparations were observed with a ZEISS Axiovert 135 microscope or a laser scanning confocal microscope. Image acquisition from the ZEISS inscribe was made with cooled CCD camera (Princeton), and the images were processed with Metamorph software (Universal Imaging Corp.).

Quantification of InlB-induced phagocytosis

In kinetic assays, in each experiment ≥100 beads or bacteria associated with 25 cells were analyzed for being extracellular or intracellular, as described previously (Braun et al., 1998), and for being associated with a discernible F-actin ring by immunofluorescence (three experiments). In internalization assays, in each experiment 100–250 beads were analyzed for being extracellular or intracellular in at least 25 transfected and 25 surrounding nontransfected cells (two to four experiments for each cell line). The score obtained in nontransfected cells was arbitrarily reported to 100, and the modification of the internalization index in the Myc-positive cells is a relative value. Results were analyzed for statistical significance using the chi-squared goodness-of-fit test ($P < 0.0001$).

Ruffles formation assays

Transfected Vero cells were starved for 5 h in DME, then stimulated or not with 4.5 nM InlB for 5 min, and fixed in 3% PFA/PBS. Immunolabeling was performed as described above. To quantify ruffling efficiency, cells that had no ruffles were scored as negative, whereas cells that had one or more ruffles were considered to be ruffle positive. In each experiment, 25 transfected and 25 surrounding nontransfected cells were analyzed (two to three experiments). The basal level of ruffle formation was not modified significantly in untreated transfected cells. In InlB-stimulated cells, the score obtained in nontransfected cells (NT) was arbitrarily reported to 100, and the modification of the ruffling index in the Myc-positive cells is a relative value. Results were analyzed for statistic significance using the chi-squared goodness-of-fit test ($P < 0.0001$).

Listeria motility assays

Vero cells were infected with the *L. monocytogenes* variant EGD-Δ*inlB*(LRRs-IR-SPA), centrifuged 1 min at 200 *g*, washed one time in DME, and incubated for 1 h. Gentamicin (10 μg/ml) was then added to kill extracellular bacteria, and cells were incubated for an additional 2 h at 37°C before fixation in 3% PFA/PBS. Immunolabelings were performed as described above. To determine the efficiency of comet tail formation, the number of total bacteria and bacteria associated with F-actin (i.e., polymerizing actin at the bacterial surface or associated with comet tails) was determined in 15 transfected cells and 15 surrounding nontransfected cells. The efficiency of tail formation is the ratio of the number of bacteria associated with actin tails to the number of all bacteria associated with F-actin. The score obtained in nontransfected cells (NT) was arbitrarily reported to 100, and the modification of the tail-forming index in the surrounding Myc-positive cells is a relative value (three independent experiments). The mean length of comet tails was determined by measuring the length of n1 tails in transfected cells and n2 tails in the neighboring nontransfected cells for 10–20 cells (n1/n2 = 80/80 for LIMK1, 12/26 for LIMK1$^-$, 50/55 for wt cofilin, and 38/96 for S3A cofilin transfection experiments) with the use of the Metamorph software (Universal Imaging Corp.).

We thank L. Braun for the strain EGDΔ*inlB*(LRRs-IR-SPA), and F. Jouneau for help in statistical analysis. We gratefully acknowledge L. Machewsky for providing plasmids pRK5-SCARWA and pRK5-SCARW, and A. Hall for providing pRK5-rac1-N17, pRK5-cdc42-N17, and pRK5-rho-N19.

This work was supported by the Ministère de l'Education Nationale et de la Recherche Scientifique et Technique (Programme PRFMMIP), the Pasteur Institute, and the GIP HMR. H. Bierne is on the Institut National de la Recherche Agronomique staff. P. Cossart is an international research scholar from the Howard Hughes Medical Institute.

Submitted: 10 April 2001
Accepted: 7 August 2001

References

Aizawa, H., Y. Fukui, and I. Yahara. 1997. Live dynamics of *Dictyostelium* cofilin suggests a role in remodeling actin latticework into bundles. *J. Cell Sci.* 110: 2333–2344.

Arber, S., F.A. Barbayannis, H. Hanser, C. Schneider, C.A. Stanyon, O. Bernard, and P. Caroni. 1998. Regulation of actin dynamics through phosphorylation of cofilin by LIM-kinase. *Nature*. 393:805–809.

Bailly, M., F. Macaluso, M. Cammer, A. Chan, J.E. Segall, and J.S. Condeelis. 1999. Relationship between Arp2/3 complex and the barbed ends of actin filaments at the leading edge of carcinoma cells after epidermal growth factor stimulation. *J. Cell Biol*. 145:331–345.

Bamburg, J.R. 1999. Proteins of the ADF/cofilin family: essential regulators of actin dynamics. *Annu. Rev. Cell Dev. Biol*. 15:185–230.

Bierne, H., S. Dramsi, M.P. Gratacap, C. Randriamampita, G. Carpenter, B. Payrastre, and P. Cossart. 2000. The invasion protein InIB from *Listeria monocytogenes* activates PLC-γ1 downstream from PI 3-kinase. *Cell. Microbiol*. 2:465–477.

Bourdet-Sicard, R., M. Rudiger, B.M. Jockusch, P. Gounon, P.J. Sansonetti, and G.T. Nhieu. 1999. Binding of the *Shigella* protein IpaA to vinculin induces F-actin depolymerization. *EMBO J*. 18:5853–5862.

Braun, L., S. Dramsi, P. Dehoux, H. Bierne, G. Lindahl, and P. Cossart. 1997. InlB: an invasion protein of *Listeria monocytogenes* with a novel type of surface association. *Mol. Microbiol*. 25:285–294.

Braun, L., H. Ohayon, and P. Cossart. 1998. The InIB protein of *Listeria monocytogenes* is sufficient to promote entry into mammalian cells. *Mol. Microbiol*. 27:1077–1087.

Braun, L., F. Nato, B. Payrastre, J.C. Mazie, and P. Cossart. 1999. The 213-amino-acid leucine-rich repeat region of the *Listeria monocytogenes* InlB protein is sufficient for entry into mammalian cells, stimulation of PI 3-kinase and membrane ruffling. *Mol. Microbiol*. 34:10–23.

Braun, L., B. Ghebrehiwet, and P. Cossart. 2000. gC1q-R/p32, a C1q-binding protein, is a receptor for the InlB invasion protein of *Listeria monocytogenes*. *EMBO J*. 19:1458–1466.

Carlier, M.F., V. Laurent, J. Santolini, R. Melki, D. Didry, G.X. Xia, Y. Hong, N.H. Chua, and D. Pantaloni. 1997. Actin depolymerizing factor (ADF/cofilin) enhances the rate of filament turnover: implication in actin-based motility. *J. Cell Biol*. 136:1307–1322.

Chan, A.Y., M. Bailly, N. Zebda, J.E. Segall, and J.S. Condeelis. 2000. Role of cofilin in epidermal growth factor-stimulated actin polymerization and lamellipod protrusion. *J. Cell Biol*. 148:531–542.

Chen, H., B.W. Bernstein, and J.R. Bamburg. 2000. Regulating actin-filament dynamics in vivo. *Trends Biochem. Sci*. 25:19–23.

Cossart, P. 2000. Actin-based motility of pathogens: the Arp2/3 complex is a central player. *Cell. Microbiol*. 3:195–205.

Cossart, P., and H. Bierne. 2001. The use of host cell machinery in the pathogenesis of *Listeria monocytogenes*. *Curr. Opin. Immunol*. 13:96–103.

Cox, D., P. Chang, Q. Zhang, P.G. Reddy, G.M. Bokoch, and S. Greenberg. 1997. Requirements for both Rac1 and Cdc42 in membrane ruffling and phagocytosis in leukocytes. *J. Exp. Med*. 186:1487–1494.

David, V., E. Gouin, M. Van Troys, A. Grogan, A.W. Segal, C. Ampe, and P. Cossart. 1998. Identification of cofilin, coronin, Rac and capZ in actin tails using a *Listeria* affinity approach. *J. Cell Sci*. 111:2877–2884.

Diakonova, M., B. Payrastre, A.G. van Velzen, W.J. Hage, P.M. van Bergen en Henegouwen, J. Boonstra, F.F. Cremers, and B.M. Humbel. 1995. Epidermal growth factor induces rapid and transient association of phospholipase C-γ1 with EGF-receptor and filamentous actin at membrane ruffles of A431 cells. *J. Cell Sci*. 108:2499–2509.

Edwards, D.C., L.C. Sanders, G.M. Bokoch, and G.N. Gill. 1999. Activation of LIM-kinase by Pak1 couples Rac/Cdc42 GTPase signalling to actin cytoskeletal dynamics. *Nat. Cell Biol*. 1:253–259.

Finlay, B.B., and P. Cossart. 1997. Exploitation of mammalian host cell functions by bacterial pathogens. *Science*. 276:718–725.

Fu, Y., and J.E. Galan. 1999. A *Salmonella* protein antagonizes Rac-1 and Cdc42 to mediate host-cell recovery after bacterial invasion. *Nature*. 401:293–297.

Gouin, E., P. Dehoux, J. Mengaud, C. Kocks, and P. Cossart. 1995. *iactA* of *Listeria ivanovii*, although distantly related to *Listeria monocytogenes actA*, restores actin tail formation in an *L. monocytogenes actA* mutant. *Infect. Immun.* 63: 2729–2737.

Ireton, K., B. Payrastre, H. Chap, W. Ogawa, H. Sakaue, M. Kasuga, and P. Cossart. 1996. A role for phosphoinositide 3-kinase in bacterial invasion. *Science*. 274:780–782 (erratum published 275:464).

Ireton, K., B. Payrastre, and P. Cossart. 1999. The *Listeria monocytogenes* protein

InlB is an agonist of mammalian phosphoinositide 3-kinase. *J. Biol. Chem*. 274:17025–17032.

Linder, S., C. Heimerl, V. Fingerle, M. Aepfelbacher, and B. Wilske. 2001. Coiling phagocytosis of *Borrelia burgdorferi* by primary human macrophages is controlled by CDC42Hs and Rac1 and involves recruitment of Wiskott-Aldrich syndrome protein and Arp2/3 complex. *Infect. Immun*. 69:1739–1746.

Kalman, D., D.D. Weiner, D.L. Goosney, J.W. Bishop. 1999. Enteropathogenic E. Coli acts through WASP and Arp2/3 complex to form pedestals. *Nat. Cell Biol*. 1:389–391.

Loisel, T.P., R. Boujemaa, D. Pantaloni, and M.F. Carlier. 1999. Reconstitution of actin-based motility of *Listeria* and *Shigella* using pure proteins. *Nature*. 401: 613–616.

Machesky, L.M., and R.H. Insall. 1998. Scar1 and the related Wiskott-Aldrich syndrome protein, WASP, regulate the actin cytoskeleton through the Arp2/3 complex. *Curr. Biol*. 8:1347–1356.

May, R.C., E. Caron, A. Hall, L.M. Machesky. 2000. Involvement of the Arp2/3 complex in phagocytosis mediated by FcγR or CR3. *Nat. Cell Biol*. 2:246–248.

Meberg, P.J., S. Ono, L.S. Minamide, M. Takahashi, and J.R. Bamburg. 1998. Actin depolymerizing factor and cofilin phosphorylation dynamics: response to signals that regulate neurite extension. *Cell Motil. Cytoskeleton*. 39:172–190.

Mengaud, J., H. Ohayon, P. Gounon, R.M. Mege, and P. Cossart. 1996a. E-cadherin is the receptor for internalin, a surface protein required for the entry of *Listeria monocytogenes* into epithelial cells. *Cell*. 84:923–932.

Mengaud, J., M. Lecuit, M. Lebrun, F. Nato, J.C. Mazie, and P. Cossart. 1996b. Antibodies to the leucine-rich repeat region of internalin block entry of *Listeria monocytogenes* into cells expressing E-cadherin. *Infect. Immun.* 64: 5430–5433.

Nagaishi, K., R. Adachi, S. Matsui, T. Yamaguchi, T. Kasahara, and K. Suzuki. 1999. Herbimycin A inhibits both dephosphorylation and translocation of cofilin induced by opsonized zymosan in macrophage-like U937 cells. *J. Cell Physiol*. 180:345–354.

Ridley, A.J., and A. Hall. 1992. The small GTP-binding protein rho regulates the assembly of focal adhesions and actin stress fibers in response to growth factors. *Cell*. 70:389–399.

Ridley, A.J., P.M. Comoglio, and A. Hall. 1995. Regulation of scatter factor/hepatocyte growth factor responses by Ras, Rac, and Rho in MDCK cells. *Mol. Cell. Biol*. 15:1110–1122.

Rosenblatt, J., B.J. Agnew, H. Abe, J.R. Bamburg, and T.J. Mitchison. 1997. *Xenopus* actin depolymerizing factor/cofilin (XAC) is responsible for the turnover of actin filaments in *Listeria monocytogenes* tails. *J. Cell Biol*. 136:1323–1332.

Royal, I., N. Lamarche-Vane, L. Lamorte, K. Kaibuchi, and M. Park. 2000. Activation of cdc42, rac, PAK, and rho-kinase in response to hepatocyte growth factor differentially regulates epithelial cell colony spreading and dissociation. *Mol. Biol. Cell*. 11:1709–1725.

Shen, Y., M. Naujokas, M. Park, and K. Ireton. 2000. InIB-dependent internalization of *Listeria* is mediated by the met receptor tyrosine kinase. *Cell*. 103: 501–510.

Stender, S., A. Friebel, S. Linder, M. Rohde, S. Mirold, and W.D. Hardt. 2000. Identification of SopE2 from *Salmonella typhimurium*, a conserved guanine nucleotide exchange factor for Cdc42 of the host cell. *Mol. Microbiol*. 36: 1206–1221.

Svitkina, T.M., and G.G. Borisy. 1999. Arp2/3 complex and actin depolymerizing factor/cofilin in dendritic organization and treadmilling of actin filament array in lamellipodia. *J. Cell Biol*. 145:1009–1026.

Tran Van Nhieu, G., A. Ben-Ze'ev, and P.J. Sansonetti. 1997. Modulation of bacterial entry into epithelial cells by association between vinculin and the *Shigella* IpaA invasin. *EMBO J*. 16:2717–2729.

Wadsworth, S.J., and H. Goldfine. 1999. *Listeria monocytogenes* phospholipase C-dependent calcium signaling modulates bacterial entry into J774 macrophage-like cells. *Infect. Immun*. 67:1770–1778.

Welch, M.D. 1999. The world according to Arp: regulation of actin nucleation by the Arp2/3 complex. *Trends Cell Biol.* 9:423–427.

Yang, N., O. Higuchi, K. Ohashi, K. Nagata, A. Wada, K. Kangawa, E. Nishida, and K. Mizuno. 1998. Cofilin phosphorylation by LIM-kinase 1 and its role in Rac-mediated actin reorganization. *Nature*. 393:809–812.

Zebda, N., O. Bernard, M. Bailly, S. Welti, D.S. Lawrence, and J.S. Condeelis. 2000. Phosphorylation of ADF/cofilin abolishes EGF-induced actin nucleation at the leading edge and subsequent lamellipod extension. *J. Cell Biol*. 151:1119–1128.